Chemistry & Biology
Article

The Differential Modulation of USP Activity by Internal Regulatory Domains, Interactors and Eight Ubiquitin Chain Types

Alex C. Faesen,[1,3] Mark P.A. Luna-Vargas,[1,3] Paul P. Geurink,[2] Marcello Clerici,[1] Remco Merkx,[2] Willem J. van Dijk,[1] Dharjath S. Hameed,[2] Farid El Oualid,[2] Huib Ovaa,[2] and Titia K. Sixma[1,*]
[1]Division of Biochemistry and Center for Biomedical Genetics
[2]Division of Cell Biology
The Netherlands Cancer Institute, Plesmanlaan 121, 1066 CX Amsterdam, The Netherlands
[3]These authors contributed equally to this work
*Correspondence: t.sixma@nki.nl
DOI 10.1016/j.chembiol.2011.10.017

SUMMARY

Ubiquitin-specific proteases (USPs) are papain-like isopeptidases with variable inter- and intramolecular regulatory domains. To understand the effect of these domains on USP activity, we have analyzed the enzyme kinetics of 12 USPs in the presence and absence of modulators using synthetic reagents. This revealed variations of several orders of magnitude in both the catalytic turnover (k_{cat}) and ubiquitin (Ub) binding (K_M) between USPs. Further activity modulation by intramolecular domains affects both the k_{cat} and K_M, whereas the intermolecular activators UAF1 and GMPS mainly increase the k_{cat}. Also, we provide the first comprehensive analysis comparing Ub chain preference. USPs can hydrolyze all linkages and show modest Ub-chain preferences, although some show a lack of activity toward linear di-Ub. This comprehensive kinetic analysis highlights the variability within the USP family.

INTRODUCTION

Since the 1980s, posttranslational modification of proteins by Ub has been the focus of many studies due to the important role of Ub in cellular processes (Hochstrasser, 2009; Pickart, 2004). Ubiquitination can mediate a multitude of signals due to its ability to form chains. It does so by using one of the seven lysine residues (K6, K11, K27, K29, K33, K48, and K63) or the N-terminal amine ("linear"), with potentially a different signal for each linkage. To counteract the effects of ubiquitination, the differential removal of Ub (chains) is carried out by deubiquitinating enzymes (DUBs).

The human genome encodes nearly 100 putative DUBs belonging to at least five subfamilies of isopeptidases (Nijman et al., 2005). The ubiquitin-specific protease (USP) family is the largest class of DUBs, with more than 60 members (Komander et al., 2009a; Nijman et al., 2005). USPs are cysteine proteases that use a papain-like mechanism to hydrolyze the isopeptide bond between the carboxy terminus of Ub and the ε-amine of the target lysine.

USPs are variable in both size and modular domain architecture, and these domains can include substrate-binding domains, ubiquitin-like (UBL) domains, and other protein-protein interaction domains (Nijman et al., 2005; Zhu et al., 2007) (Figure 1A). They share a common papain-like fold, but the catalytic domains can have large insertions (Ye et al., 2009), possibly directly affecting activity, Ub binding, or localization as seen in USP4 (Luna-Vargas et al., 2011b), USP5 (Reyes-Turcu et al., 2008), USP14 (Borodovsky et al., 2001), and CYLD (Komander et al., 2008). In addition, some USPs need structural rearrangements to bind their substrate and catalyze hydrolysis (Avvakumov et al., 2006; Hu et al., 2002; Hu et al., 2005; Köhler et al., 2010; Samara et al., 2010).

USPs are often found in large protein complexes, and many interaction partners of USPs have been identified (Sowa et al., 2009). Although the function of most interaction partners is still unclear, some play a role in the modulation of USP activity. For example, GMP synthetase (GMPS) interacts and activates USP7 (Faesen et al., 2011; Sarkari et al., 2009; van der Knaap et al., 2005), whereas the WD40 repeat containing UAF1 (WDR48) activates USP1, USP12, and USP46 (Cohn et al., 2007, 2009).

With its diversity of domain architectures, internal insertions within the catalytic domain, and external modulators, the USP family apparently requires different levels of regulation. This poses a number of unanswered questions. For instance, what is the variability of the activity between the catalytic domains and the full-length proteins? Are there preferences for Ub-chain types, and does this change in the presence of external modulators?

To address these questions, we have developed and produced (El Oualid et al., 2010) chemical tools and used them to characterize a set of 12 USPs. This revealed variations of several orders of magnitude in catalytic turnover and Ub binding and allowed characterization of intra- and intermolecular activity modulation. We determined the chain preferences of all USPs against all eight topoisomers. This showed modest chain specificity among the di-ubiquitin linkages that was variable between USPs. We observe activity toward all topoisomers, except for some USPs that are inactive toward linear di-ubiquitin. These preferences did not change in the presence of the modulators. Kinetic analysis of the hydrolysis showed that there is no additional Ub binding site, suggesting that the chain preferences are achieved by steric hindrance or reduced catalytic turnover.

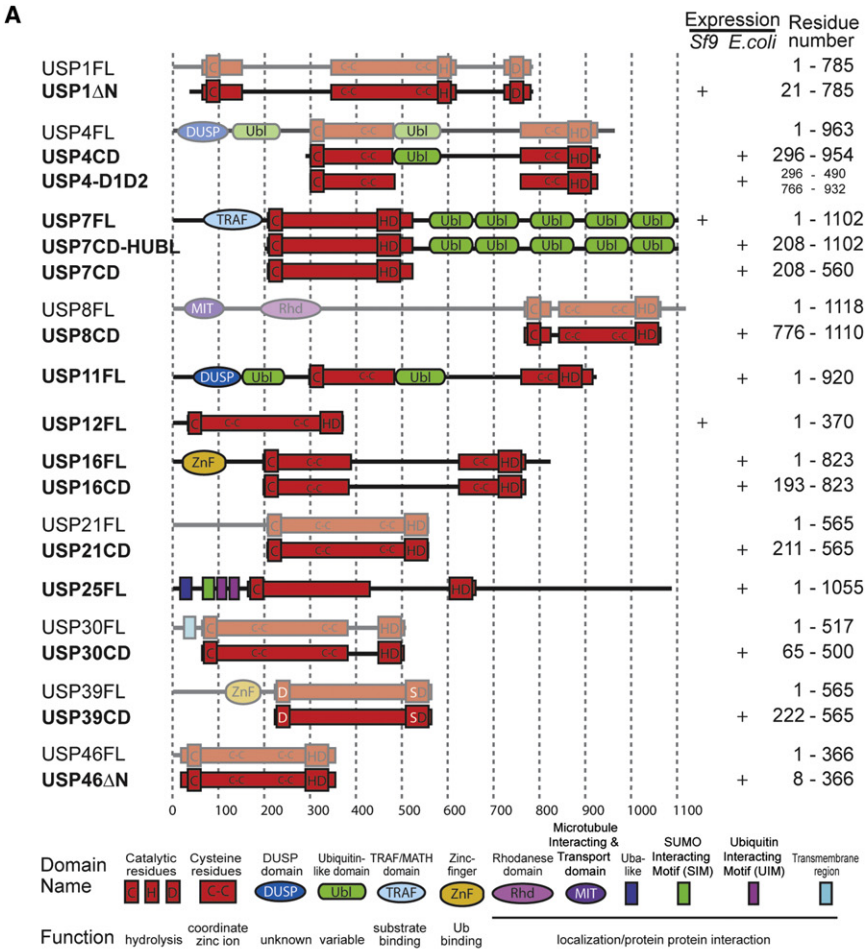

Figure 1. Overview of the Characterized USPs

(A) Domain architecture of the USPs used in this study. The constructs used in this manuscript are highlighted with corresponding residue numbers and expression system.

(B) Final purification product of the USP constructs shown on SDS-PAGE gel. An asterisk indicates the expressed USP. USP7FL has an N-terminal GST tag.

Related to Table S1.

RESULTS

Protein Cloning, Expression, and Purification

Based on protein expression trials (Luna-Vargas et al., 2011a), we identified constructs suitable for large-scale protein expression of 12 different USPs in either *E. coli* or *Sf9* insect cells (Figure 1A). In this study, we could therefore include 16 constructs containing either the (almost) full-length constructs (USP1ΔN, USP7FL, USP11FL, USP12FL, USP16FL, USP25FL, and USP46ΔN, with ΔN and ΔC denoting N- and C-terminal truncations, respectively), or the catalytic domain (USP4CD, USP7CD, USP8CD, USP16CD, USP21CD, USP30CD, and USP39CD) (Figures 1A and 1B). In addition, we expressed and purified two known USP activity modulators: UAF1 (Cohn et al., 2007) and GMPS (van der Knaap et al., 2005). Cloning, expression, and purification protocols are provided in the Materials and Methods section.

Large Variations in Both Catalytic Turnover and Ub Binding

Although USP family members share a homologous catalytic domain, many contain insertions within their catalytic domain or have additional domains with the potential to influence their activity (Luna-Vargas et al., 2011b; Ye et al., 2009) (Figure 1A). To study these effects, we determined the kinetic parameters of all the USPs we have available. To this end, we produced a minimal synthetic Ub substrate fused at its C-terminus to the small molecule 7-amino-4-methylcoumarin (UbAMC) (Dang et al., 1998; El Oualid et al., 2010). The UbAMC substrate is a reagent widely used to assay DUB activity. Upon hydrolysis by the DUB, the free AMC reporter molecule produces a fluorescent signal that allows for a direct read-out of activity (Figure S1A available online). The presence of the AMC moiety instead of the endogenous target makes this into a minimal universal substrate.

This assay is performed in the presence of EDTA to prevent inhibition by divalent cations (Fernández-Montalván et al., 2007). Since this might affect the structural integrity of the zinc-containing USPs (Figure 1), we also determined the relative activity without EDTA (Figure S1B). The activity of all USPs except USP30CD is unaffected. Here, the catalytic turnover is decreased 2.5-fold upon addition of EDTA (Figure S1C). The activity of USP30CD without EDTA is shown in Figure 2.

Overall, we observed variations of several orders of magnitude in both K_M and k_{cat} between the USP constructs (Figure 2). Previously published kinetic parameters of USPs are listed in

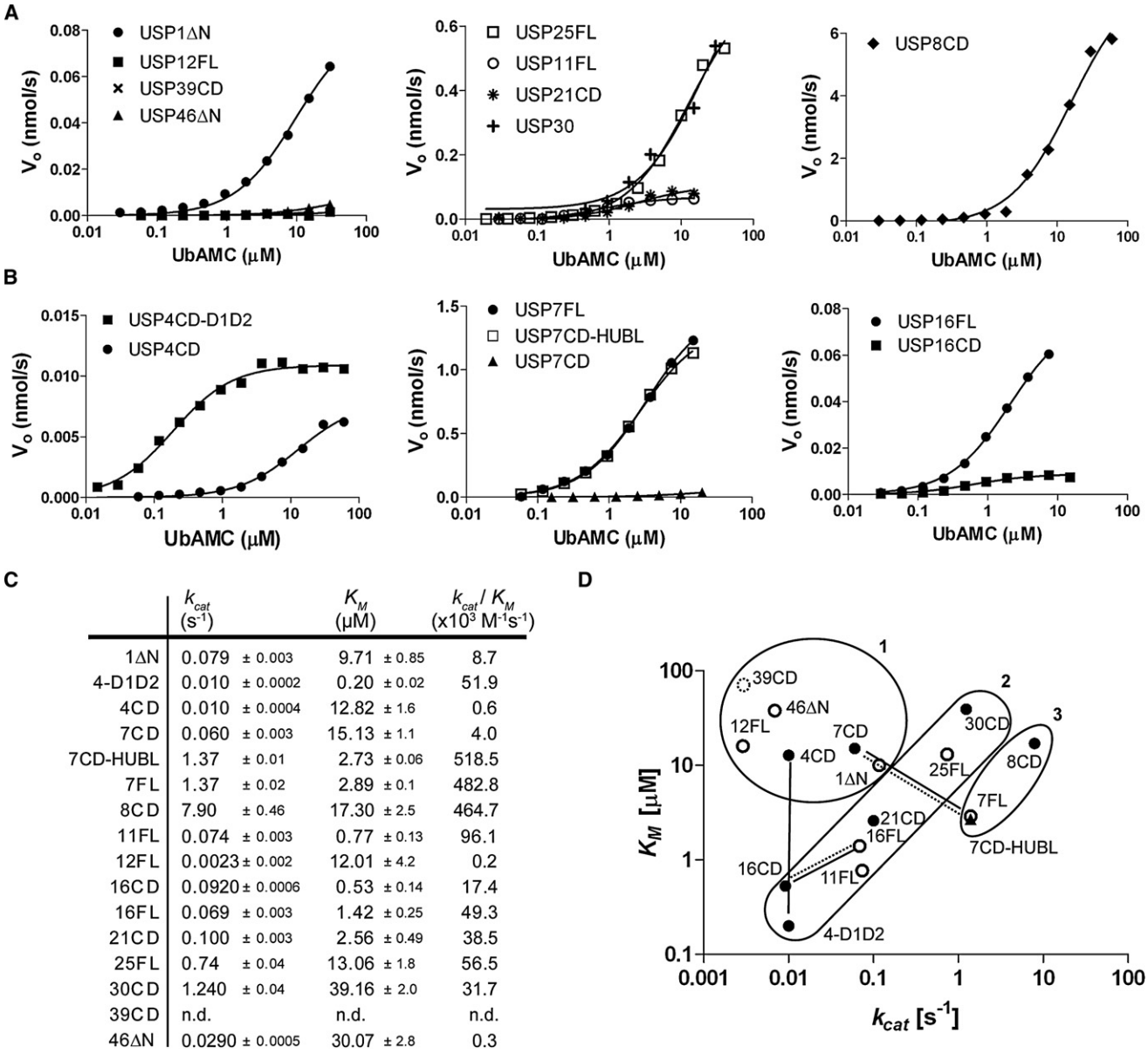

C

	k_{cat} (s^{-1})	K_M (μM)	k_{cat}/K_M (x10^3 $M^{-1}s^{-1}$)
1ΔN	0.079 ± 0.003	9.71 ± 0.85	8.7
4-D1D2	0.010 ± 0.0002	0.20 ± 0.02	51.9
4CD	0.010 ± 0.0004	12.82 ± 1.6	0.6
7CD	0.060 ± 0.003	15.13 ± 1.1	4.0
7CD-HUBL	1.37 ± 0.01	2.73 ± 0.06	518.5
7FL	1.37 ± 0.02	2.89 ± 0.1	482.8
8CD	7.90 ± 0.46	17.30 ± 2.5	464.7
11FL	0.074 ± 0.003	0.77 ± 0.13	96.1
12FL	0.0023 ± 0.002	12.01 ± 4.2	0.2
16CD	0.0920 ± 0.0006	0.53 ± 0.14	17.4
16FL	0.069 ± 0.003	1.42 ± 0.25	49.3
21CD	0.100 ± 0.003	2.56 ± 0.49	38.5
25FL	0.74 ± 0.04	13.06 ± 1.8	56.5
30CD	1.240 ± 0.04	39.16 ± 2.0	31.7
39CD	n.d.	n.d.	n.d.
46ΔN	0.0290 ± 0.0005	30.07 ± 2.8	0.3

Figure 2. Kinetic Parameters Using UbAMC

(A and B) Michaelis-Menten curves for the different USPs, obtained by determining the initial rates (V_0) at different UbAMC concentrations, and for USPs with intramolecular modulation (B). The assay was performed in duplicate.

(C) Overview of the kinetic parameters (k_{cat}, K_M, and k_{cat}/K_M) for the different USPs. Values for USP4 and USP7 are from Luna-Vargas et al. (2011b) and Faesen et al. (2011), respectively.

(D) Activity classification of USPs, based on kinetic parameters, where group 1 represents the USPs with the lowest activity; group 2 contains USPs with intermediate activity, and group 3 contains the USPs with the highest activity. Dashed lines link the catalytic domains with the corresponding full-length USPs. Solid lines show the effect of intramolecular activating and inhibiting domains.

Related to Figure S1.

Table S1. This substrate allows direct comparison of relative activity among the USP family members. This resulted in a rough classification in three groups based on the kinetic parameters (Figure 2D). Group 1 represents the USPs whose activity is very limited due to a low k_{cat} (USP1ΔN, USP4CD, USP7CD, USP12FL, USP39CD, and USP46ΔN). The ''intermediate'' group, group 2, contains the USPs that show moderate activity (USP4-D1D2, USP11FL, USP16CD, USP16FL, USP21CD, USP25FL, and USP30CD), and group 3 contains very active USPs (USP7FL, USP7CD-HUBL, and USP8CD).

As expected, group 1 contains USP39CD. It shows no activity, since it lacks the catalytic cysteine and histidine residues (Nijman et al., 2005). Group 1 also contains USP1ΔN, USP12FL, and USP46ΔN, all three known to have low activity, which is

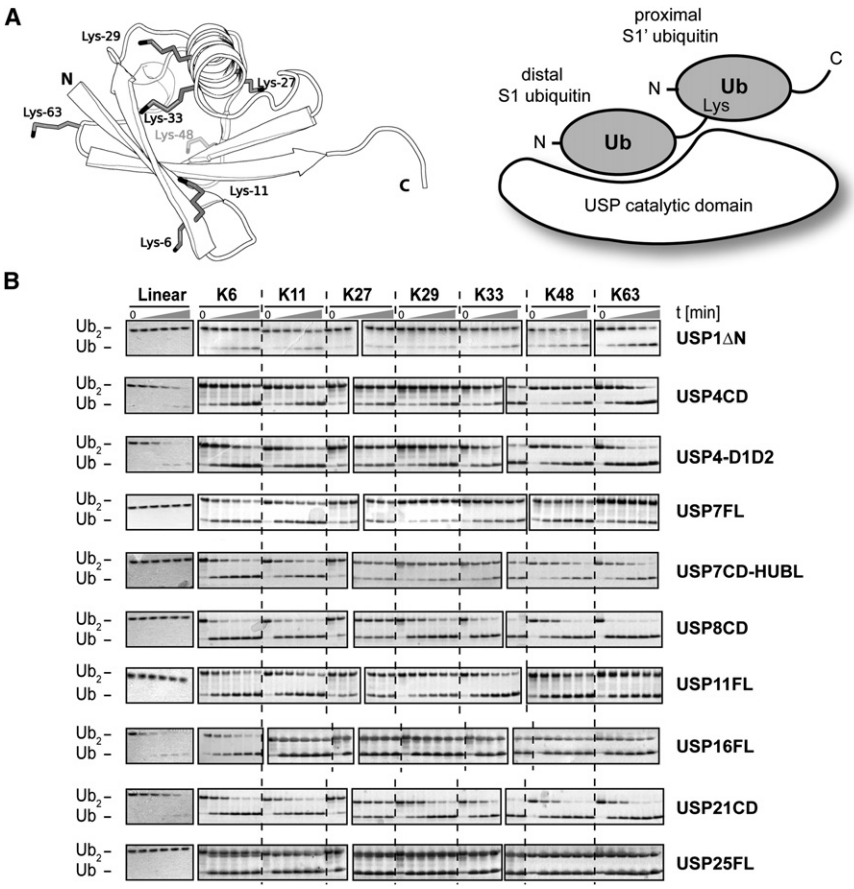

Figure 3. Di-Ub Topoisomer Preference for the Different USPs

(A) Ub (1UBQ) Showing all Lysines.

(B) Overview of a time-course using all eight different di-Ub topoisomers (5 μM) (Linear, K6, K11, K27, K29, K33, K48, and K63) for the active USPs (75 nM). Samples from each time point (0, 5, 10, 30, 60, and 180 min) were analyzed on Coomassie-stained SDS-PAGE gels. The assay was performed twice, and representative gels are shown here.

Related to Figure S2.

enhanced by the external modulator UAF1 (Cohn et al., 2009; Cohn et al., 2007).

In contrast, group 3 represents the most active USPs, and contains both USP8CD and the USP7 constructs with activating C-terminal Hausp UBL (HUBL) domain (Faesen et al., 2011). Interestingly, USP8CD has an unusually weak K_M, possibly due to an inserted α-helix in the catalytic domain, which is suggested to stabilize the observed closed conformation (Avvakumov et al., 2006). However, this is compensated by a very high catalytic turnover, rendering it a very active USP overall.

Intramolecular Modulation of USP Activity

Not only do we observe differences in enzymatic behavior between the USPs, but we also observe differential effects of intramolecular domains on the activity of the (minimal) catalytic domains in USP4, USP7, and USP16 (Figure 2B).

We recently showed that USP4 contains a UBL domain inserted in its catalytic domain (USP4CD; Figure 1A), which inhibits the activity of USP4CD (group 1; Figures 2B and 2D) (Luna-Vargas et al., 2011b; Zhu et al., 2007). The presence of this UBL domain in USP4CD increases the K_M and is therefore less active than the minimal catalytic domain USP4-D1D2 (group 2; Figure 2D) (Luna-Vargas et al., 2011b). In contrast, both k_{cat} and K_M are affected in USP7, where the minimal catalytic domain (group 1) shows far less activity than the full-length enzyme (group 3). Here, the activity of USP7 is modulated by its HUBL domain, which is essential for both activity and Ub binding in vitro and in vivo (Faesen et al., 2011; Fernández-Montalván et al., 2007; Ma et al., 2010). The activity of USP16CD is modulated by the zinc-finger Ub specific protease (ZnF-UBP) domain. Surprisingly, the activity is enhanced by increasing catalytic turnover, rather than by the K_M (Figures 2B and 2D). Since it is a Ub-binding domain, the effect of the zinc-finger could be more prominent in poly-Ub processing (Pai et al., 2007), which might add up to a bigger difference than observed here. USP39CD also contains a Znf-UBP domain, but it is unlikely that this will lead to enzymatic activation since USP39CD does not have the catalytic residues.

Overall, this shows that several intramolecular domains are able to modulate USPs. The modulation can affect K_M (USP4), k_{cat} (USP16), or both (USP7), and both inhibitory and activating domains are found in USPs. Together, this creates an additional layer of regulation of the catalytic activity of USPs.

Di-Ub Preferences of USPs

Most studies of DUB specificity have focused on processing K48- and K63-linked poly-Ub. K48-linked ubiquitination targets a protein for active degradation by the proteasome (Chau et al., 1989), whereas ubiquitin chains using K63 have mostly nondegradative outcomes (Chen and Sun, 2009). Our knowledge of functions of the other linkages is growing. For example, linear ubiquitin chains play a role in the NFκB activation pathway and immune response and are structurally similar to K63-linked poly-Ub (Gerlach et al., 2011; Komander et al., 2009b; Tokunaga et al., 2009). K11 is also a strong degradation signal and is involved in the cell cycle (Williamson et al., 2009). The roles of the other linkages remain elusive, but they have been implicated in DNA damage response (K6 by BRCA1/BARD1 (Wu-Baer et al., 2003)) or lysosomal degradation (K29 (Chastagner et al., 2006, 2008)).

Since the additional linkages serve important cellular functions, we synthesized all seven lysine-linked di-Ub topoisomers (El Oualid et al., 2010). Together with linear di-ubiquitin we used them in a qualitative assay to assess all linkage preferences of the panel of USPs (Figure 3 and Figure S2). Previously published

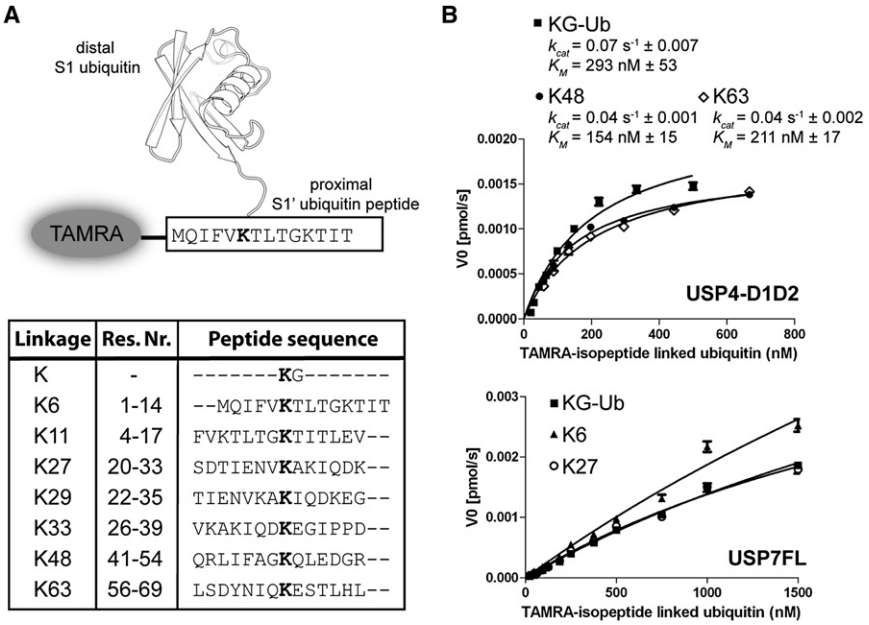

Linkage	Res. Nr.	Peptide sequence
K	-	-------KG-------
K6	1-14	--MQIFVKTLTGKTIT
K11	4-17	FVKTLTGKTITLEV--
K27	20-33	SDTIENVKAKIQDK--
K29	22-35	TIENVKAKIQDKEG--
K33	26-39	VKAKIQDKEGIPPD--
K48	41-54	QRLIFAGKQLEDGR--
K63	56-69	LSDYNIQKESTLHL--

Figure 4. Isopeptide-Linked Ubiquitin FP-Reagents

(A) Schematic view of N-terminal TAMRA-labeled Ub peptide (K6) conjugated with Ub. Table shows the peptide sequences used with the corresponding residue numbers for the different types of Ub linkage. The conjugated lysine is highlighted. (B) Michaelis-Menten curves for USP4-D1D2 (*top*) and USP7FL (*bottom*) were obtained using the TAMRA-labeled Ub peptides in an FP hydrolysis assay. The curves for USP7 could not be fitted. The assay was performed in triplicate.
Related to Figure S3.

preferences are corroborated (Song et al., 2010; Ye et al., 2011). Overall, the relative activities from the UbAMC assay are retained, with a few exceptions. For example, USP21CD shows only intermediate activity in the UbAMC assay, but it displays activities in the di-Ub assay almost matching the most active USP, USP8CD.

The USP family seems to be rather promiscuous compared to other DUB families. For example, the OTU family displays strong linkage preferences for specific di-Ub topoisomers (Bremm et al., 2010; Edelmann et al., 2009; Virdee et al., 2010; Wang et al., 2009). Figure 3 shows that the differential activity of the USPs is smaller. Most of the active USPs from this study hydrolyze all di-Ub topoisomers. Nevertheless, there are clear differences in efficiency. For instance, although USP1ΔN, USP7, USP8CD, USP11FL, and USP25FL showed robust activity toward the lysine-linked di-Ub topoisomers, we observe no activity toward linear di-Ub. On the other hand, USP4, USP16FL, and USP21CD are active against linear di-Ub. Of these three, USP21CD is the only one that is less active against the linear di-Ub compared to the other topoisomers. The hydrolysis of linear di-Ub is unique for the USP family, since this feature is not observed in other DUB families (Komander, 2010).

Also in the hydrolysis of the lysine-linked topoisomers we observe differential activity. For instance, most USPs have difficulties hydrolyzing K27- and, to a lesser extent, K29-linked di-Ub. USP7 has limited activity toward hydrolyzing K27- and K29-linked di-Ub. In contrast, the K6, K11, K48, and K63 Ub topoisomers are hydrolyzed relatively efficiently. Another clear example is USP4, for which K63-linked di-Ub is a better substrate than K48-linked di-Ub (Luna-Vargas et al., 2011b; Song et al., 2010).

We wondered whether the intramolecular modulating domains in USP4, USP7, and USP16 change the linkage preferences. The different USPs respond differently to modulation by internal domains, analogous to what was observed with UbAMC (Figures 3, S2B, and S2C). However, no change in linkage preference was seen between catalytic domain and longer constructs, showing that the modulation effects are substrate-independent mechanisms.

Overall, this shows that in contrast to other DUB families, USPs can hydrolyze all di-Ub topoisomers, albeit with differences in catalytic efficiency. Also, some USPs show perturbed activity toward linear-linked ubiquitin. The differences in catalytic efficiency are preserved in the presence of the intramolecular activity modulators.

In the Case of USPs, Isopeptide-Linked Ub Is Not Representative for di-Ub

To explain the Ub linkage preference, we might not need full-length di-Ub (Shanmugham et al., 2010). To test this in an activity assay, we designed and synthesized a panel of fluorescence polarization-based (FP) reagents that mimic the lysine-linked di-Ubs. In these reagents, TAMRA-labeled Ub peptides were linked via an isopeptide linkage to the carboxy terminus of wild-type full-length mono-Ub (Tirat et al., 2005) (Figures 4A and S3)). Therefore, in contrast to the peptide linkage in UbAMC, these FP reagents use the natural isopeptide linkage. The proximal Ub is represented by 14-mer peptides, each representing one of the seven lysines of Ub (Figures 3A and 4A). In addition, a di-peptide (KG) was prepared to serve as a minimal substrate. Mass spectrometry and SDS-PAGE analysis of these new Ub substrates showed that the synthesis was successful for all eight different TAMRA-labeled isopeptide-linked Ub FP reagents (Figures S3C and S3F).

As a proof of principle, we used the minimal "KG" FP reagent to determine the kinetic parameters of USP4-D1D2 (Figures 4B and S4H). With this reagent we determined K_M (293 nM) and k_{cat} (0.07 s^{-1}) values similar to the kinetic parameters obtained using UbAMC. Only the k_{cat} is higher, possibly due to the difference in the chemical nature of the linkage, since the FP reagents contain a natural isopeptide linkage in contrast to the UbAMC reagent. However, since the K_M values are similar, both represent comparable Ub reagents.

In the di-Ub time course assay, we observed linkage preferences of USP4-D1D2 and USP7; e.g., USP7 prefers the hydrolysis of K6- over K27-linked di-Ub, and USP4-D1D2 prefers K63- over K48-linked di-Ub (Figure 3). Although difficult to fit for USP7, with our FP reagents we observed no difference in

activity for either USP4-D1D2 or USP7 and therefore could not recapitulate the preferences observed in the di-Ub assay (Figures 4B, S3G, and S3H). This shows that these FP reagents do not contain the information required to mimic di-Ub for USPs.

The Proximal Ub Hinders Binding to USP7 and USP21 in Specific Linkages

Since the FP reagents were not sufficient to reproduce the observed linkage preference, we used full-length di-Ubs to determine the kinetic parameters directly. We determined K_M and k_{cat} of the hydrolysis of all di-Ubs by USP7 and USP21, using gel-based initial rate experiments that monitored the appearance of mono-Ub (Figure 5). These assays reproduced the differences observed in the time course assay (Figure 3). For USP7, the kinetic parameters were similar to the UbAMC assay (2.9 μM and 1.37 s^{-1} in the UbAMC assay), but for USP21CD, the k_{cat} is 7- to 8-fold higher in the di-Ub assay (0.1 s^{-1} with UbAMC). The K_M is not tighter in the di-Ub assay compared to the UbAMC (roughly 3 μM compared to 2.56 μM with UbAMC), suggesting that there is no induced binding or catalysis effect by the proximal Ub moiety.

These experiments showed that the linkages that are most efficiently hydrolyzed by USP7 and USP21 (K6, K11, K33, K48, and K63) have similar kinetic behavior (Figures 5B and 5C). In the initial di-Ub assay, the K27, K29, and linear linkages showed a clear delayed hydrolysis by USP7 and USP21 (Figure 3). This was nicely reproduced in this kinetic di-Ub assay (Figures 5 and S4). Interestingly, for K27 and K29 for both USPs, there was hardly any change in k_{cat}; rather, the K_M increased far above the concentrations used in our assays. This suggests that the preference for the di-Ub topoisomers arises from steric hindrance rather than an additional binding site for the proximal Ub moiety. Apparently, the binding of some linkages to the catalytic domain is impaired, resulting in lower activity.

The linear di-Ub is a particularly bad substrate for USP7. Also, in the kinetic analysis, no hydrolysis is observed, even when using up to 15 μM of substrate (Figure 5A). On the other hand, USP21CD is active toward linear di-Ub. The kinetic analysis showed that both the k_{cat} and the K_M are reduced compared to those of the other di-Ub topoisomers. This suggests a decreased capacity to hydrolyze peptide bonds compared to isopeptide bonds, with possibly a reduced binding as well.

Intermolecular Activation of USPs by UAF1 and GMPS Only Affects k_{cat}

Besides their intrinsic activity, some USPs are activated by intermolecular modulation. For example, USP1, USP12, and USP46 are activated by the WD40-repeat containing UAF1, and USP7 is activated by GMPS (Cohn et al., 2007, 2009; Faesen et al., 2011; van der Knaap et al., 2005). Here, we used the UbAMC assay to quantify this activation (Figures 6A, 6B, and S4). In agreement with previous data, we observe mainly a k_{cat} increase (7-fold) of USP1ΔN activity in the presence of UAF1. The USP1 used in this work has a mutation in the self-cleavage site (Gly671,672Ala) (Cohn et al., 2007). UAF1 also activates USP12FL and USP46ΔN, where the k_{cat} is increased by 66- and 70-fold, respectively. Also, in the case of USP7, we observed a k_{cat} increase (5.5-fold) in the presence of its modulator GMPS. Interestingly, in contrast to variable modulation invoked by internal domains (Figure 2D), intermolecular modulation is achieved mainly by an increase in the catalytic turnover rather than in substrate binding (Figure 6B).

To investigate whether this activation also induces new linkage preferences of these USPs, we repeated the di-Ub assay in the presence of UAF1 or GMPS (Figure 6C). As expected from the UbAMC kinetics, USP1ΔN shows limited activity in the absence of UAF1, and USP12FL and USP46CD show no activity. However, in the presence of UAF1, the activity of all three USPs is increased, albeit not to the same level. In complex with their activators, USP1ΔN and USP7CD-HUBL show the most activity, but no change in chain-type preference by UAF1 or GMPS. This agrees well with an activation mechanism that only increases k_{cat}, but does not induce binding, which should translate to changing K_M values.

DISCUSSION

In this study, we used novel reagents to determine the kinetic parameters of substrate-independent activity of 12 USPs, their di-Ub linkage preferences, and characteristics of both intra- and intermolecular activity modulation. We observe large variations in both the catalytic turnover (k_{cat}) and Ub binding (K_M) between USPs. This variability in activity can be explained in several ways. First, the activity can be affected by structural rearrangements in both Ub binding sites and active sites, as shown by structural studies (Avvakumov et al., 2006; Hu et al., 2002). Second, intramolecular domains of USPs can modulate the DUB activity, as seen here for USP4, USP7, and USP16. External modulator proteins can further regulate the activity of the USP by enhancing its activity, as seen for USP1, USP7, USP12, and USP46 (Figure 6).

Here, we characterize a few cases where intramolecular modulators regulate the USP catalytic efficiency: either insertions within or additional domains outside the catalytic domain. For both USP7 and USP16 the enzymatic behavior is regulated by intramolecular domains (the HUBL and ZnF-UBP domains, respectively) outside the catalytic domain, resulting in the increase of the activity. In addition, variations in kinetics can be induced by (large) insertions in the catalytic domains themselves, as demonstrated for USP4, where a UBL-containing insert inhibits the catalytic efficiency (Luna-Vargas et al., 2011b). These variations and intramolecular modulations result in the unique activity of each USP.

For the last decade, the main focus on DUB specificity for Ub chains has been on K48- and K63-linked poly-Ub chains. However, different Ub linkage topoisomers can result in different cellular fates, some of which are very specific (Jin et al., 2008; Matsumoto et al., 2010; Wu et al., 2010) and require a minimal chain length to invoke its function (Cook et al., 1994; Thrower et al., 2000). Our study presents the first complete and comprehensive study on di-Ub preference of all eight linkages for USP family members. Also, with our (mainly) synthetic di-Ub substrate, we confirm earlier reports on preferences (Song et al., 2010; Ye et al., 2011). Although none of the DUBs so far has been tested for all Ub linkages, some DUBs show remarkable specificity (Cooper et al., 2009; Edelmann et al., 2009; Kayagaki et al., 2007; McCullough et al., 2004; Wang et al., 2009). Next to CYLD (Komander et al., 2008), the USPs do not have

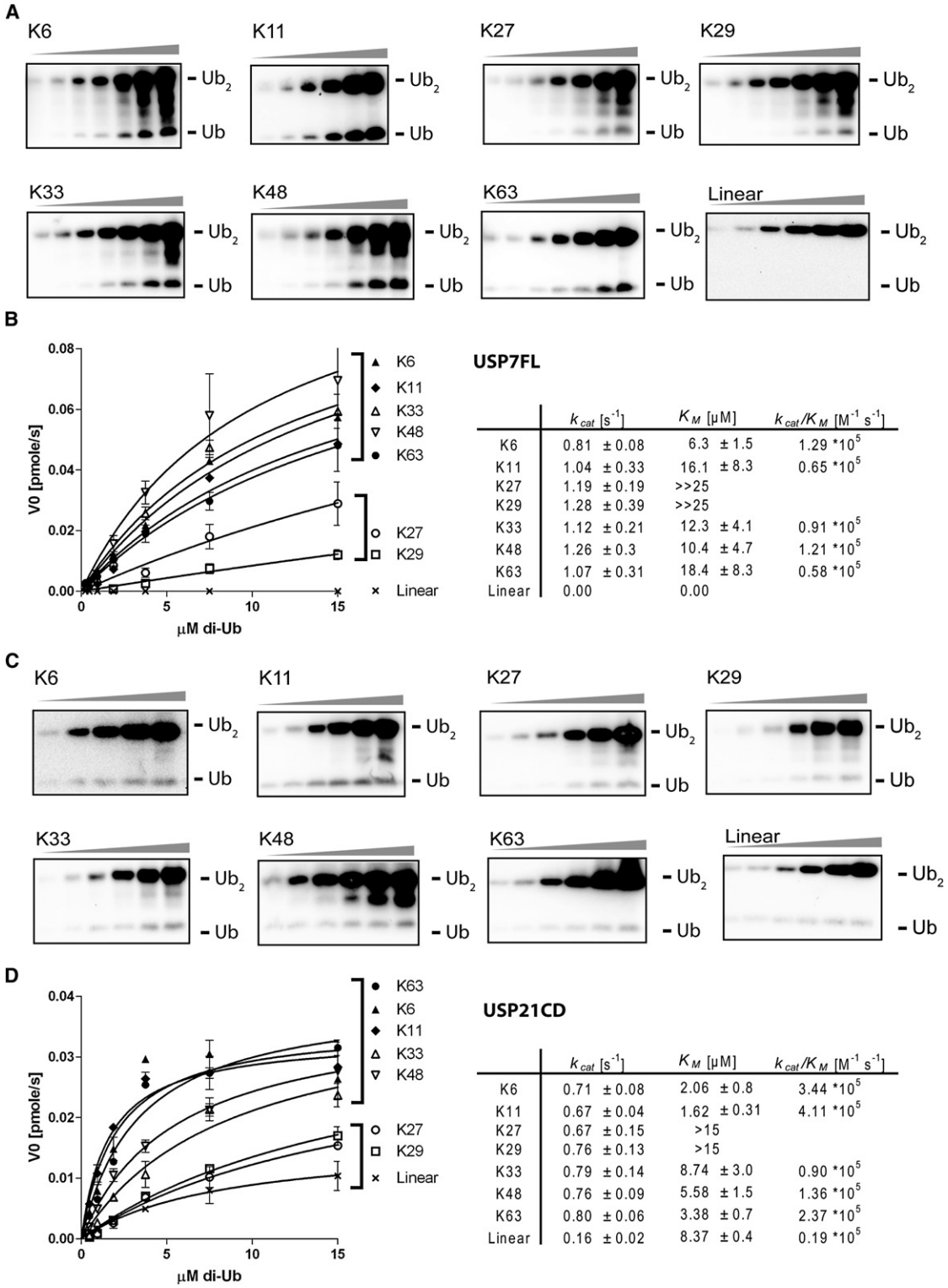

	k_{cat} [s^{-1}]	K_M [μM]	k_{cat}/K_M [M^{-1} s^{-1}]
K6	0.81 ± 0.08	6.3 ± 1.5	1.29 *10^5
K11	1.04 ± 0.33	16.1 ± 8.3	0.65 *10^5
K27	1.19 ± 0.19	>>25	
K29	1.28 ± 0.39	>>25	
K33	1.12 ± 0.21	12.3 ± 4.1	0.91 *10^5
K48	1.26 ± 0.3	10.4 ± 4.7	1.21 *10^5
K63	1.07 ± 0.31	18.4 ± 8.3	0.58 *10^5
Linear	0.00	0.00	

	k_{cat} [s^{-1}]	K_M [μM]	k_{cat}/K_M [M^{-1} s^{-1}]
K6	0.71 ± 0.08	2.06 ± 0.8	3.44 *10^5
K11	0.67 ± 0.04	1.62 ± 0.31	4.11 *10^5
K27	0.67 ± 0.15	>15	
K29	0.76 ± 0.13	>15	
K33	0.79 ± 0.14	8.74 ± 3.0	0.90 *10^5
K48	0.76 ± 0.09	5.58 ± 1.5	1.36 *10^5
K63	0.80 ± 0.06	3.38 ± 0.7	2.37 *10^5
Linear	0.16 ± 0.02	8.37 ± 0.4	0.19 *10^5

Figure 5. Michaelis-Menten Kinetics of di-Ub Hydrolysis by USP7FL and USP21CD

(A and C) Representative western blots of the Michaelis-Menten analysis of di-Ub hydrolysis by USP7FL (A) and USP21CD (C). Assay was performed using 2-fold dilutions of the di-Ub starting at 15 μM for 5 min at 37°C.

(B and D) Michaelis-Menten analysis for USP7FL (B) and USP21CD (D) for di-ubiquitin hydrolysis. Initial rate (V_0) of di-Ub conversion into mono-Ub was determined at different substrate concentration from western blots shown in (A). The conversion to mono-Ub was quantified using the unsaturated di-Ub signal corrected for conversion. The assay was perfomed in duplicate.

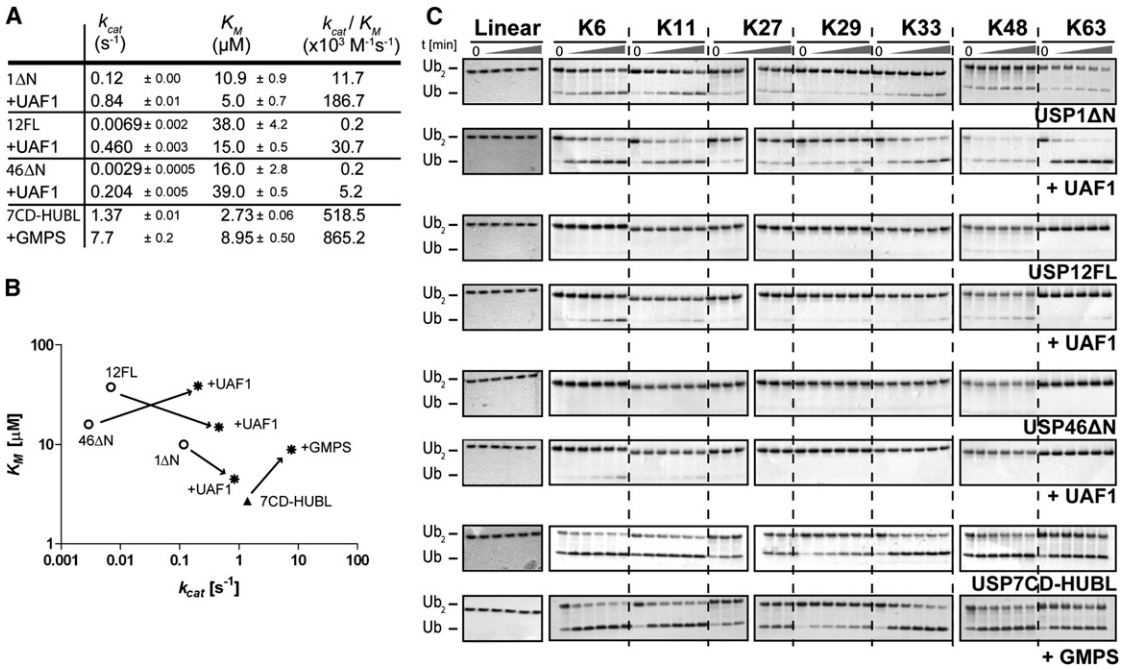

Figure 6. Intermolecular USP Activity Modulation Is Achieved by Increasing k_{cat}

(A) Kinetic parameters (k_{cat}, K_M, and k_{cat}/K_M) using UbAMC as the substrate for USP1ΔN, USP12FL, and USP46ΔN in the presence of UAF1 and USP7CD-HUBL in the presence of GMPS. The assay was performed in duplicate.

(B) Graphical comparison of the kinetic parameters comparing the USP activity between the USPs and in the presence of their modulator.

(C) Activity modulation by UAF1 and GMPS toward all eight di-Ub topoisomers. The USP concentration used was 75 nM. Samples from each time point (0, 5, 10, 30, 60, and 180 min) were analyzed on Coomassie-stained SDS-PAGE gels.

Related to Figure S4.

strict chain-type specificity, but rather have preferences. Kinetic analysis of the hydrolysis by USP7 and USP21 showed us that there is no proximal S1′ Ub binding site to induce Ub topoisomer preference; rather, the proximal Ub moiety induces steric constraints for binding to the USP in the case of K27 or K29 linkages. These linkage preferences might be increased when using longer Ub chains, since some might be ordered in higher-order structures (Bremm et al., 2010; Tenno et al., 2004; Varadan et al., 2002).

Overall, the hydrolysis efficiency of the USPs toward K6-, K11-, K48-, and K63-linked Ub was higher than for K27- and, to a lesser extent, K29- and K33-linked di-Ub. These residues localize in distinct regions on Ub (Figure 3A). The lysine residues involved in the most easily hydrolyzed linkages (K6, K11, K48, and K63) are in the β-sheet or loops. In contrast, the lysine residues of the more difficult linkages (K27, K29, and K33) are positioned on the other side of the Ub molecule, and are all in the α1-helix. In addition, K27 is barely accessible, which possibly induces a steric constraint, resulting in the lower activity. This interesting property needs future investigation.

Compared to the other DUB families, the USPs display a more promiscuous behavior and some are able to hydrolyze all Ub topoisomers with modest differences. For some USPs, the activity toward linear di-Ub is slower or even completely lost (Figures 3B and 5A). There are several possible explanations. First, there is a difference in chemistry due to the lower pKa of the N-terminal amine (9.2) compared to the ε-amine of lysine (10.5). Second, the peptide bond in linear di-Ub is conformationally more restrained compared to the more flexible isopeptide lysine linkage. Finally, the large side chain of the N-terminal methionine introduces steric hindrance in the (“linear”) peptide bond. Any of these aspects could influence binding and/or catalytic efficiency of the hydrolysis of the peptide bond. Still, DUBs from the other families are not able to hydrolyze linear-linked Ub chains, and therefore the USP family is the only known family with members that can process this linkage type.

A previous study suggested that Ub-peptide reagents might be sufficient to discriminate between topoisomers in binding (Shanmugham et al., 2010). However, in our activity assays with the FP Ub-peptide reagents, we observed no difference between Ub linkages. This suggests that the peptides do not contain enough information to mimic the proximal Ub for the USPs. Nevertheless, they may be sufficient for DUBs from families with more pronounced Ub specificity and be useful tools in those cases.

In our di-Ub assays, some USPs seemed more active compared to the UbAMC assay. For example, USP7 was one of the most active substrates in the UbAMC assay, whereas in the di-Ub assay, this activity was matched by USP11 and USP16. In our kinetic analysis of the di-Ub hydrolysis, we observe no changes in catalytic parameters for USP7, which shows that this enzyme does not differentiate between the two substrates. This subsequently shows that several other USPs are more active against di-Ub, which is an endogenous

substrate, compared to UbAMC. Therefore, our KG FP reagent could prove a good alternative for UbAMC, since it contains the natural isopeptide linkage, which is not present in UbAMC. Using the KG FP reagent with USP4-D1D2 and USP21CD shows a slightly higher k_{cat} compared to UbAMC (Figures 4B and S3I). Therefore, this suggests that for some USPs the KG FP reagent may be a better substrate, and provide more relevant kinetic parameters.

This study confirmed that the modulator UAF1 activates USP1, USP12, and USP46, and GMPS activates USP7. This activation occurs mainly by increasing the k_{cat}. However, the biological roles of the UAF1 and GMPS activation are distinct. UAF1 activation is almost essential for USP activity of USP1, USP12, and USP46. This resembles the Ubp8 activation by Sgf11 (Köhler et al., 2010; Samara et al., 2010). Surprisingly, USP12 in complex with UAF1 is still not very active, possibly requiring additional partners, like WDR20 (Kee et al., 2010). In a different manner, GMPS hyperactivates USP7, by allosterically stabilizing the active state of the enzyme induced by the HUBL domain (Faesen et al., 2011). Besides this general activation, the GMPS activity modulation most likely has additional substrate-specific roles, as it induces histone H2B deubiquitination (van der Knaap et al., 2005).

Although the functions of an increasing number of USPs have been elucidated, they still represent a relatively uncharacterized enzyme family. To aid in the biochemical understanding of these enzymes, we here report large variations in kinetics and intramolecular modulation (k_{cat} and K_M) and a characterization of the activation by intermolecular interactions (k_{cat}). Although some USPs show a lack of activity toward linear di-Ub, it is the only DUB family with members that can hydrolyze all topoisomers with a modest but surprising differential activity. The combined data provide insights in the variation in the biochemical behavior of the USP enzyme family.

SIGNIFICANCE

Ubiquitination is a dynamic process that is involved in numerous key cellular processes. The removal of the Ub molecules is an integral part of this process and is carried out by deubiquitinating enzymes (DUBs). These are increasingly recognized as interesting drug targets. However, to date, we lack the markers to predict the biochemical behavior based on sequence alignments, and therefore, a need exists for comprehensive kinetic studies. This is where chemical tools that allow fast and accurate readouts will contribute to answering these biological questions. In this study, we designed and produced several such chemical reagents to determine the kinetics and di-Ub linkage preferences of 12 USPs. Despite the homologous catalytic domain, the kinetic data underline the large variability within the USP family, and the intra- and intermolecular activity modulators create an additional layer of regulation.

In addition, this study for the first time reports the linkage preference of 12 USPs against all possible di-Ubs. This family represents the first DUB family that can hydrolyze all di-Ub topoisomers, albeit with small differential activity. Kinetic analysis of the hydrolysis of the di-Ub topoisomers suggests that within the USP family some of the preferences are induced by steric hindrance rather than induced binding, as seen in other DUB families.

Together, these data provide insight into the biochemical behavior in the USP family and validate the chemical tools that now also can be applied in characterizing other DUB families.

EXPERIMENTAL PROCEDURES

General

General reagents were obtained from Sigma Aldrich, Fluka, and Acros and used as received. Solvents were purchased from Biosolve or Aldrich. Peptide synthesis reagents were purchased from Novabiochem. cDNA of USP1, USP12, USP46, and UAF1 were obtained from Martin A. Cohn and Alan D'Andrea, USP4 and USP8 from Annette Dirac and Rene Bernards, USP21 and USP39 from Elisabetta Citterio, USP30 from Carlos Lopex-Otin, and USP25 from Erik Meulmeester and Frauke Melchior. Linear di-Ub was purchased from Boston Biochem.

General Plasmids and Proteins

Di-Ub moieties were produced as previously described (El Oualid et al., 2010). USP4CD (aa 296–954), USP4-D1D2 (aa 296–490/766–932), USP8CD (aa 776–1110), USP11FL (aa 1–920), USP16FL (aa 1–823), USP16CD (aa 193–823), USP21CD (aa 211–565), USP30CD (aa 65–500), USP39CD (aa 222–565), and USP46ΔN (aa 8–366) are cloned into the pETNKI-LIC vector for expression in bacteria as described (Luna-Vargas et al., 2011a). USP1ΔN (aa 21–785 self-cleavage site glycine 671 and 672 are mutated to alanine), USP7FL (aa 1–1102), USP12FL (aa 1–355) and STREP-TEV-UAF1 (aa 6–677) are cloned into the pFastBac-HTb vector for expression in insect cells. Both USP7CD-HUBL (aa 208–1102) and USP7CD (aa 208–560) are cloned into the pGEX vector (Faesen et al., 2011), and USP25FL is cloned in the pET11a vector (Meulmeester et al., 2008). Codon-optimized full-length USP7 and GMPS cDNA was obtained from DomainEx (Cambridge, UK). Genes USP7 and GMPS were both PCR-amplified and subcloned (SpeI/NotI) into a pFastBac vector (Invitrogen) containing an N-terminal GST tag (BamHI/SpeI) and Prescission Protease cleavage site. cDNA for USP11 and USP16 was obtained from ImaGenes (Berlin, Germany).

Protein Expression and Purification

As specified in Figure 1, the USPs were expressed in both *E. coli* and insect cells and purified as described (Faesen et al., 2011; Luna-Vargas et al., 2011a). GMPS was expressed and purified as before (Faesen et al., 2011). Depending on the type of vector, the tag was removed with either TEV or the HRV 3C protease. Bacmids were prepared following the manufacturer's guidelines. USP1, USP12, and UAF1 were produced using *Sf9* and *Sf21* insect cell expression. Infection was done using a low-MOI infection protocol (Fitzgerald et al., 2006). The cells were harvested 72 hr after a baculovirus-induced growth arrest was observed. USP46 was produced in *E. coli*. USP1, USP12, USP46, and UAF1 were purified using Ni^{2+} sepharose (GE Healthcare, Waukesha, WI) in 20 mM HEPES (pH 7.5), 150 mM NaCl, 0.1 mM PMSF, and 0.1 mM DTT followed by elution using imidazole. His-tag was removed by overnight cleavage with TEV protease while dialyzing to remove imidazole. Uncleaved product was removed with Ni^{2+} sepharose. Size exclusion chromatography was performed using a Superdex 200 or 75 column (GE Healthcare), equilibrated against buffer containing 10 mM HEPES (pH 7.5) 100 mM NaCl, and 1 mM DTT. All proteins were concentrated to ~10 mg/ml and stored at −80°C.

UbAMC Assay

Kinetics was determined as described before (Luna-Vargas et al., 2011b). The activity was assayed at 25°C in 50 mM HEPES buffer (pH 7.5), 100mM NaCl, 1 mM EDTA, 5 mM DTT, and 0.05% (w/v) Tween-20. Assays were performed in nonbinding surface, flat-bottom, low-flange black 384-well plates (Corning) in a 30 μl reaction volume. Fluorescence was measured at 5-min intervals using a Fluostar Optima plate reader (BMG Labtechnologies, de Meern, The Netherlands) at excitation and emission wavelengths of 355 nm and 460 nm, respectively. All replicate assays were performed simultaneously in duplicates. USP concentration varied between 1 and 100 nM, depending on relative

activity. The hydrolysis rate was linear for at least 1 hr, and corrected for background signal (no enzyme). UAF1 and GMPS were added in a 1:1 stoichiometry. USPs were added immediately before the first measurement. In order to calculate the kinetic parameters for the hydrolysis of UbAMC, curves were obtained by plotting the measured enzyme initial rates (v) versus the corresponding substrate concentrations ([S]). These were subjected to nonlinear regression fit using the Michaelis-Menten equation $V = (Vmax \times [S])/([S] + K_M)$ (Equation 1), where Vmax is the maximal velocity at saturating substrate concentrations and K_M the Michaelis constant. The k_{cat} value was derived from the equation $k_{cat} = Vmax/[Eo]$ (Equation 2), where [Eo] is the total enzyme concentration. Experimental data were processed using Prism 5.01 (GraphPad Software).

Di-Ub Assay

Di-Ub hydrolysis reactions were performed at 37°C in 50 mM HEPES buffer at pH 7.5, with 100 mM NaCl, 1 mM EDTA, 5 mM dithiothreitol, and 0.05% (w/v) Tween-20 with constant enzyme concentration (75 nM). When indicated, UAF1 was added in a 2-fold excess (150 nM) and GMPS in a 1:1 stoichiometry. Experiments were performed using several preps of the di-Ub topoisomers, some containing small amounts (<5%) of mono-Ub. The kinetics assays were performed using the cleanest samples. Reactions were stopped by addition of SDS loading buffer and followed by SDS-PAGE analysis. The time course assay (Figure 3) has been repeated at least two times. For the kinetic analysis, the reaction mixture was preheated to 37°C degrees before adding USP7. Samples were run on a 12% Bis-Tris NuPage gel (duplicates on one gel), and western blots were performed with anti-Ub antibody (Santa Cruz, CA; P4D1). The ChemiDoc system (Biorad) was used to read the chemiluminence signal. Quantification of mono-Ub was done using the quantification tools of ImageLab (Biorad) using a marker of known amount of mono-Ub and the non-saturated di-Ub signal (including a correction for the amount of di-Ub converted to mono-Ub). Experimental data were processed using Prism 5.01 (GraphPad Software).

Solid-Phase Peptide Synthesis of the TAMRA Thiolysine Peptides

Solid-phase peptide synthesis (SPPS) of the TAMRA thiolysine peptides was performed on a Syro II MultiSyntech Automated Peptide synthesizer using standard 9-fluorenylmethoxycarbonyl (Fmoc)-based solid-phase peptide chemistry at 25 μmol scale, using fourfold excess of amino acids relative to preloaded Fmoc amino acid Wang type resin (0.2 mmol/g, Applied Biosystems). The following protected amino acids were used during Ub peptide synthesis: Fmoc-L-Ala-OH, Fmoc-L-Arg- (Pbf)-OH, Fmoc-L-Asn (Trt)-OH, Fmoc-L-Asp (O*t*Bu)-OH, Fmoc-L-Gln (Trt)-OH, Fmoc-L-Glu (OtBu)-OH, Fmoc-Gly-OH, Fmoc-L-His (Trt)-OH, Fmoc-L-Ile-OH, Fmoc-L-Leu-OH, Fmoc-L-Lys (Boc)-OH, Fmoc-L-Met-OH; Fmoc-L-Phe-OH; Fmoc-L-Pro-OH; Fmoc-L-Ser (*t*Bu)-OH; Fmoc-L-Thr (*t*Bu)-OH, Fmoc-L-Tyr (*t*Bu)-OH, and Fmoc-L-Val-OH. Fmoc-5*S*-(methyldisulfanyl)-(L)-Lys (Boc)-OH was synthesized as described previously (El Oualid et al., 2010).

The coupling procedure starts off with single couplings in N-methylpyrrolidon (NMP) for 45 min using PyBOP (4 equiv) and DiPEA (12 equiv) in a total volume of 750 μl. This is followed by removal of Fmoc with 20% piperidine in NMP for 2 × 2 and 1 × 5 min. The procedure ends with NMP wash steps after each coupling (3 times) and deprotection (5 times).

The resin was washed with diethylether and dried under high vacuum. Next, the polypeptide sequence was detached from the resin and deprotected by treatment with TFA/H_2O/Phenol/iPr_3SiH 90.5:5:2.5:2 v/v/v/v for 2.5 hr. After washing the resin with 3 × 1 ml TFA, the crude protein was precipitated with cold Et_2O/*n*-pentane 3:1 v/v. The precipitated protein was washed 3 times with diethylether; the pellet was dissolved in a mixture of H_2O/CH_3CN/HOAc (65:25:10 v/v/v) and finally lyophilized. All peptides were analyzed by LC-MS and purified by RP-HPLC when necessary.

LC-MS

LC-MS measurements on the FP reagents or components thereof were performed on a Waters (Milford, MA) 2795 Separation Module (Alliance HT), equipped with a Waters 2996 Photodiode Array Detector (190-750nm), Phenomenex Kinetex C18 column (2.1 × 50, 2.6 μm), and LCT orthogonal acceleration time-of-flight mass spectrometer. Samples were run using two mobile phases: A, 0.1% formic acid in water; and B, 0.1% formic acid in acetonitrile. Flow rate, 0.8 ml/min; runtime, 6 min; column T, 40°C. Gradient: 0–0.5 min, 5% B; 0.5–4 min: 5%–95% B; 4–5.5 min, 95% B. Data processing was performed using Waters MassLynx Mass Spectrometry Software 4.1 (deconvolution with Maxent1 function).

Ligation of Ub to the Peptides Followed by Desulphurization

Schematic overview of reaction scheme to create final FP reagents and the corresponding final yields can be found in Figure S3. A mixture of 4-mercaptophenylacetic acid (MPAA, 100 mM) and TCEP (50 mM) in 6 M guanidinium·HCl (1 ml, pH 7) was added to Ub-MesNa thioester (5 mg, prepared according to the procedure described previously (El Oualid et al., 2010). To this the TAMRA thiolysine peptide (100 μl of a 20 mM stock solution in DMSO) was added and the whole mixture was incubated at 37°C. After overnight incubation, all low-molecular-weight material was removed using a 3-kDa cutoff spin-column (Amicon Ultra) in four centrifuge cycles. The crude material was taken up in 6 M guanidinium·HCl and 0.1 M sodium phosphate (4 ml, pH 6.5), and to this was added TCEP (187 mg) and glutathione (30 mg), after which the pH of the mixture was adjusted to pH 6.5 by addition of 1 M NaOH. Next, the mixture was degassed with argon, after which radical initiator VA-044 was added. The mixture was incubated at 37°C overnight. All constructs were purified by RP-HPLC and analyzed by LC-MS and gel electrophoresis and were obtained as purple solids.

C18 RP-HPLC

Purification of the FP reagents by RP-HPLC was performed on a Shimadzu system equipped with an LC-20AT liquid chromatography pump, CTO-20A column oven (T = 40°C), SPD-20A UV/VIS detector (detection simultaneously at 230 nm and 254 nm), RF-10AXL fluorescence detector (ex/em = 540/600 nm), and Atlantis Prep T3 column (10 × 150 mm, 5 μm). Samples were run using two mobile phases: A, 0.05% trifluoroacetic acid in water; and B, 0.05% trifluoroacetic acid in acetonitrile. Flow rate, 7.5 ml/min; runtime, 30 min. Gradient: 0–6 min: 5%–10% B; 6.5–26 min: 25%–47% B; 26.5–29.5 min: 95% B. Pure fractions were pooled and lyophilized.

Isopeptide-Linked Ub FP Hydrolysis Assay

FP assays were performed on a PerkinElmer Wallac EnVision 2010 Multilabel Reader with a 531 nm excitation filter and two 579 nm emission filters. The confocal optics were adjusted with TAMRA-KG (synthesized by SPPS as described above) and the G factor was determined using a polarization value for TAMRA-KG (25 nM) of 50 mP. The assays were performed in nonbinding-surface, flat-bottom, low-flange black 384-well plates (Corning) at room temperature in a buffer containing 20 mM Tris·HCl, pH 7.5, 5 mM DTT, 100 mM NaCl, 1 mg/ml 3-[(3-cholamidopropyl) dimethylammonio] propanesulfonic acid (CHAPS), and 0.5 mg/ml bovine gamma globulin (BGG). Each well had a volume of 20 μl. Buffer and enzyme were predispensed and the reaction was started by the addition of substrate. Kinetic data were collected at intervals of 2.5 or 3 min. First measurement was taken a few minutes after the start of the reaction. From the obtained polarization values (P) the amount of processed substrate (P_t) was calculated according to the following equation (Levine et al., 1997): $S = S_0 - S_0 \cdot ((P_t - P_{min})/(P_{max} - P_{min}))$, where P_t is the polarization measured (in mP); P_{max} is the polarization of 100% unprocessed substrate (determined for every reagent at all used substrate concentrations); P_{min} is the polarization of 100% processed substrate (determined for every linkage at all used substrate concentrations by measuring the mP value for the corresponding deubiquitinated TAMRA-peptide, which were synthesized by SPPS according to the procedure described above); and S_0 is the amount of substrate added to the reaction. From the obtained P_t values the values for initial velocities were calculated, and these values were used to determine the Michaelis-Menten constants. These were linear for at least 30 min and corrected for background signal (no enzyme). All experimental data was processed using MS Excel and Prism 4.03 (GraphPad Software).

SUPPLEMENTAL INFORMATION

Supplemental Information includes one table and four figures and can be found with this article online at doi:10.1016/j.chembiol.2011.10.017.

ACKNOWLEDGMENTS

We thank Martin A. Cohn and Alan D'Andrea for USP1, USP12, USP46, and UAF1 ccDNA, Annette Dirac and Rene Bernards for USP4 and USP8 cDNA, Elisabetta Citterio for USP21 and USP39 cDNA, Carlos Lopex-Otin for USP30 cDNA, and Erik Meulmeester and Frauke Melchior for USP25 cDNA. We thank Ovaa and Sixma group members for discussion, sharing reagents, and critical reading of the manuscript. This work was supported by grants from the Dutch Cancer Society, the Netherlands Organization for Scientific Research (VIDI grant), and EU-Rubicon and NWO-CW ECHO 700.59.009, KWF-2008-4014, and STW.

USP expression and purification were performed by M.P.A.L.V. with assistance from W.J.v.D; enzyme assays were designed and analyzed by A.C.F. and executed by M.P.A.L.V and A.C.F.; USP1, USP12, USP46, and UAF1 were expressed, purified, and analyzed by M.C.; UbAMC was designed and synthesized by R.M.; di-Ubs were designed by F.E. and H.O. and synthesized by D.S.H.; FP reagents were designed by F.E., P.P.G., and H.O. and synthesized by P.P.G. and F.E.; FP reagent assays were performed by P.P.G.; H.O. supervised all synthesis efforts and FP experiments; T.K.S. designed and supervised the USP project; data analysis and manuscript writing were by A.C.F. with M.P.A.L.V. and T.K.S.

Received: July 1, 2011
Revised: October 11, 2011
Accepted: October 31, 2011
Published: December 22, 2011

REFERENCES

Avvakumov, G.V., Walker, J.R., Xue, S., Finerty, P.J., Jr., Mackenzie, F., Newman, E.M., and Dhe-Paganon, S. (2006). Amino-terminal dimerization, NRDP1-rhodanese interaction, and inhibited catalytic domain conformation of the ubiquitin-specific protease 8 (USP8). J. Biol. Chem. *281*, 38061–38070.

Borodovsky, A., Kessler, B.M., Casagrande, R., Overkleeft, H.S., Wilkinson, K.D., and Ploegh, H.L. (2001). A novel active site-directed probe specific for deubiquitylating enzymes reveals proteasome association of USP14. EMBO J. *20*, 5187–5196.

Bremm, A., Freund, S.M., and Komander, D. (2010). Lys11-linked ubiquitin chains adopt compact conformations and are preferentially hydrolyzed by the deubiquitinase Cezanne. Nat. Struct. Mol. Biol. *17*, 939–947.

Chastagner, P., Israël, A., and Brou, C. (2006). Itch/AIP4 mediates Deltex degradation through the formation of K29-linked polyubiquitin chains. EMBO Rep. *7*, 1147–1153.

Chastagner, P., Israël, A., and Brou, C. (2008). AIP4/Itch regulates Notch receptor degradation in the absence of ligand. PLoS ONE *3*, e2735.

Chau, V., Tobias, J.W., Bachmair, A., Marriott, D., Ecker, D.J., Gonda, D.K., and Varshavsky, A. (1989). A multiubiquitin chain is confined to specific lysine in a targeted short-lived protein. Science *243*, 1576–1583.

Chen, Z.J., and Sun, L.J. (2009). Nonproteolytic functions of ubiquitin in cell signaling. Mol. Cell *33*, 275–286.

Cohn, M.A., Kowal, P., Yang, K., Haas, W., Huang, T.T., Gygi, S.P., and D'Andrea, A.D. (2007). A UAF1-containing multisubunit protein complex regulates the Fanconi anemia pathway. Mol. Cell *28*, 786–797.

Cohn, M.A., Kee, Y., Haas, W., Gygi, S.P., and D'Andrea, A.D. (2009). UAF1 is a subunit of multiple deubiquitinating enzyme complexes. J. Biol. Chem. *284*, 5343–5351.

Cook, W.J., Jeffrey, L.C., Kasperek, E., and Pickart, C.M. (1994). Structure of tetraubiquitin shows how multiubiquitin chains can be formed. J. Mol. Biol. *236*, 601–609.

Cooper, E.M., Cutcliffe, C., Kristiansen, T.Z., Pandey, A., Pickart, C.M., and Cohen, R.E. (2009). K63-specific deubiquitination by two JAMM/MPN+ complexes: BRISC-associated Brcc36 and proteasomal Poh1. EMBO J. *28*, 621–631.

Dang, L.C., Melandri, F.D., and Stein, R.L. (1998). Kinetic and mechanistic studies on the hydrolysis of ubiquitin C-terminal 7-amido-4-methylcoumarin by deubiquitinating enzymes. Biochemistry *37*, 1868–1879.

Edelmann, M.J., Iphöfer, A., Akutsu, M., Altun, M., di Gleria, K., Kramer, H.B., Fiebiger, E., Dhe-Paganon, S., and Kessler, B.M. (2009). Structural basis and specificity of human otubain 1-mediated deubiquitination. Biochem. J. *418*, 379–390.

El Oualid, F., Merkx, R., Ekkebus, R., Hameed, D.S., Smit, J.J., de Jong, A., Hilkmann, H., Sixma, T.K., and Ovaa, H. (2010). Chemical synthesis of ubiquitin, ubiquitin-based probes, and diubiquitin. Angew. Chem. Int. Ed. Engl. *49*, 10149–10153.

Faesen, A.C., Dirac, A.M., Shanmugham, A., Ovaa, H., Perrakis, A., and Sixma, T.K. (2011). Mechanism of USP7/HAUSP activation by its C-terminal ubiquitin-like domain and allosteric regulation by GMP-synthetase. Mol. Cell *44*, 147–159.

Fernández-Montalván, A., Bouwmeester, T., Joberty, G., Mader, R., Mahnke, M., Pierrat, B., Schlaeppi, J.M., Worpenberg, S., and Gerhartz, B. (2007). Biochemical characterization of USP7 reveals post-translational modification sites and structural requirements for substrate processing and subcellular localization. FEBS J. *274*, 4256–4270.

Fitzgerald, D.J., Berger, P., Schaffitzel, C., Yamada, K., Richmond, T.J., and Berger, I. (2006). Protein complex expression by using multigene baculoviral vectors. Nat. Methods *3*, 1021–1032.

Gerlach, B., Cordier, S.M., Schmukle, A.C., Emmerich, C.H., Rieser, E., Haas, T.L., Webb, A.I., Rickard, J.A., Anderton, H., Wong, W.W., et al. (2011). Linear ubiquitination prevents inflammation and regulates immune signalling. Nature *471*, 591–596.

Hochstrasser, M. (2009). Origin and function of ubiquitin-like proteins. Nature *458*, 422–429.

Hu, M., Li, P., Li, M., Li, W., Yao, T., Wu, J.W., Gu, W., Cohen, R.E., and Shi, Y. (2002). Crystal structure of a UBP-family deubiquitinating enzyme in isolation and in complex with ubiquitin aldehyde. Cell *111*, 1041–1054.

Hu, M., Li, P., Song, L., Jeffrey, P.D., Chenova, T.A., Wilkinson, K.D., Cohen, R.E., and Shi, Y. (2005). Structure and mechanisms of the proteasome-associated deubiquitinating enzyme USP14. EMBO J. *24*, 3747–3756.

Jin, L., Williamson, A., Banerjee, S., Philipp, I., and Rape, M. (2008). Mechanism of ubiquitin-chain formation by the human anaphase-promoting complex. Cell *133*, 653–665.

Kayagaki, N., Phung, Q., Chan, S., Chaudhari, R., Quan, C., O'Rourke, K.M., Eby, M., Pietras, E., Cheng, G., Bazan, J.F., et al. (2007). DUBA: a deubiquitinase that regulates type I interferon production. Science *318*, 1628–1632.

Kee, Y., Yang, K., Cohn, M.A., Haas, W., Gygi, S.P., and D'Andrea, A.D. (2010). WDR20 regulates activity of the USP12 x UAF1 deubiquitinating enzyme complex. J. Biol. Chem. *285*, 11252–11257.

Köhler, A., Zimmerman, E., Schneider, M., Hurt, E., and Zheng, N. (2010). Structural basis for assembly and activation of the heterotetrameric SAGA histone H2B deubiquitinase module. Cell *141*, 606–617.

Komander, D. (2010). Mechanism, specificity and structure of the deubiquitinases. Subcell. Biochem. *54*, 69–87.

Komander, D., Lord, C.J., Scheel, H., Swift, S., Hofmann, K., Ashworth, A., and Barford, D. (2008). The structure of the CYLD USP domain explains its specificity for Lys63-linked polyubiquitin and reveals a B box module. Mol. Cell *29*, 451–464.

Komander, D., Clague, M.J., and Urbe, S. (2009a). Breaking the chains: structure and function of the deubiquitinases. Nat. Rev. *10*, 550–563.

Komander, D., Reyes-Turcu, F., Licchesi, J.D., Odenwaelder, P., Wilkinson, K.D., and Barford, D. (2009b). Molecular discrimination of structurally equivalent Lys 63-linked and linear polyubiquitin chains. EMBO Rep. *10*, 466–473.

Levine, L.M., Michener, M.L., Toth, M.V., and Holwerda, B.C. (1997). Measurement of specific protease activity utilizing fluorescence polarization. Anal. Biochem. *247*, 83–88.

Luna-Vargas, M.P., Christodoulou, E., Alfieri, A., van Dijk, P., Stadnik, M., Hibbert, R.G., Sahtoe, D.D., Clerici, M., Marco, V.D., Littler, D., et al. (2011a). Enabling high-throughput ligation-independent cloning and protein expression for the family of ubiquitin specific proteases. J. Struct. Biol. *175*, 113–119.

Luna-Vargas, M.P., Faesen, A.C., van Dijk, W.J., Rape, M., Fish, A., and Sixma, T.K. (2011b). Ubiquitin-specific protease 4 is inhibited by its ubiquitin-like domain. EMBO Rep. *12*, 365–372.

Ma, J., Martin, J.D., Xue, Y., Lor, L.A., Kennedy-Wilson, K.M., Sinnamon, R.H., Ho, T.F., Zhang, G., Schwartz, B., Tummino, P.J., and Lai, Z. (2010). C-terminal region of USP7/HAUSP is critical for deubiquitination activity and contains a second mdm2/p53 binding site. Arch. Biochem. Biophys. *503*, 207–212.

Matsumoto, M.L., Wickliffe, K.E., Dong, K.C., Yu, C., Bosanac, I., Bustos, D., Phu, L., Kirkpatrick, D.S., Hymowitz, S.G., Rape, M., et al. (2010). K11-linked polyubiquitination in cell cycle control revealed by a K11 linkage-specific antibody. Mol. Cell *39*, 477–484.

McCullough, J., Clague, M.J., and Urbé, S. (2004). AMSH is an endosome-associated ubiquitin isopeptidase. J. Cell Biol. *166*, 487–492.

Meulmeester, E., Kunze, M., Hsiao, H.H., Urlaub, H., and Melchior, F. (2008). Mechanism and consequences for paralog-specific sumoylation of ubiquitin-specific protease 25. Mol. Cell *30*, 610–619.

Nijman, S.M., Luna-Vargas, M.P., Velds, A., Brummelkamp, T.R., Dirac, A.M., Sixma, T.K., and Bernards, R. (2005). A genomic and functional inventory of deubiquitinating enzymes. Cell *123*, 773–786.

Pai, M.T., Tzeng, S.R., Kovacs, J.J., Keaton, M.A., Li, S.S., Yao, T.P., and Zhou, P. (2007). Solution structure of the Ubp-M BUZ domain, a highly specific protein module that recognizes the C-terminal tail of free ubiquitin. J. Mol. Biol. *370*, 290–302.

Pickart, C.M. (2004). Back to the future with ubiquitin. Cell *116*, 181–190.

Reyes-Turcu, F.E., Shanks, J.R., Komander, D., and Wilkinson, K.D. (2008). Recognition of polyubiquitin isoforms by the multiple ubiquitin binding modules of isopeptidase T. J. Biol. Chem. *283*, 19581–19592.

Samara, N.L., Datta, A.B., Berndsen, C.E., Zhang, X., Yao, T., Cohen, R.E., and Wolberger, C. (2010). Structural insights into the assembly and function of the SAGA deubiquitinating module. Science *328*, 1025–1029.

Sarkari, F., Sanchez-Alcaraz, T., Wang, S., Holowaty, M.N., Sheng, Y., and Frappier, L. (2009). EBNA1-mediated recruitment of a histone H2B deubiquitylating complex to the Epstein-Barr virus latent origin of DNA replication. PLoS Pathog. *5*, e1000624.

Shanmugham, A., Fish, A., Luna-Vargas, M.P., Faesen, A.C., El Oualid, F., Sixma, T.K., and Ovaa, H. (2010). Nonhydrolyzable ubiquitin-isopeptide isosteres as deubiquitinating enzyme probes. J. Am. Chem. Soc. *132*, 8834–8835.

Song, E.J., Werner, S.L., Neubauer, J., Stegmeier, F., Aspden, J., Rio, D., Harper, J.W., Elledge, S.J., Kirschner, M.W., and Rape, M. (2010). The Prp19 complex and the Usp4Sart3 deubiquitinating enzyme control reversible ubiquitination at the spliceosome. Genes Dev. *24*, 1434–1447.

Sowa, M.E., Bennett, E.J., Gygi, S.P., and Harper, J.W. (2009). Defining the human deubiquitinating enzyme interaction landscape. Cell *138*, 389–403.

Tenno, T., Fujiwara, K., Tochio, H., Iwai, K., Morita, E.H., Hayashi, H., Murata, S., Hiroaki, H., Sato, M., Tanaka, K., and Shirakawa, M. (2004). Structural basis for distinct roles of Lys63- and Lys48-linked polyubiquitin chains. Genes Cells *9*, 865–875.

Thrower, J.S., Hoffman, L., Rechsteiner, M., and Pickart, C.M. (2000). Recognition of the polyubiquitin proteolytic signal. EMBO J. *19*, 94–102.

Tirat, A., Schilb, A., Riou, V., Leder, L., Gerhartz, B., Zimmermann, J., Worpenberg, S., Eidhoff, U., Freuler, F., Stettler, T., et al. (2005). Synthesis and characterization of fluorescent ubiquitin derivatives as highly sensitive substrates for the deubiquitinating enzymes UCH-L3 and USP-2. Anal. Biochem. *343*, 244–255.

Tokunaga, F., Sakata, S., Saeki, Y., Satomi, Y., Kirisako, T., Kamei, K., Nakagawa, T., Kato, M., Murata, S., Yamaoka, S., et al. (2009). Involvement of linear polyubiquitylation of NEMO in NF-kappaB activation. Nat. Cell Biol. *11*, 123–132.

van der Knaap, J.A., Kumar, B.R., Moshkin, Y.M., Langenberg, K., Krijgsveld, J., Heck, A.J., Karch, F., and Verrijzer, C.P. (2005). GMP synthetase stimulates histone H2B deubiquitylation by the epigenetic silencer USP7. Mol. Cell *17*, 695–707.

Varadan, R., Walker, O., Pickart, C., and Fushman, D. (2002). Structural properties of polyubiquitin chains in solution. J. Mol. Biol. *324*, 637–647.

Virdee, S., Ye, Y., Nguyen, D.P., Komander, D., and Chin, J.W. (2010). Engineered diubiquitin synthesis reveals Lys29-isopeptide specificity of an OTU deubiquitinase. Nat. Chem. Biol. *6*, 750–757.

Wang, T., Yin, L., Cooper, E.M., Lai, M.Y., Dickey, S., Pickart, C.M., Fushman, D., Wilkinson, K.D., Cohen, R.E., and Wolberger, C. (2009). Evidence for bidentate substrate binding as the basis for the K48 linkage specificity of otubain 1. J. Mol. Biol. *386*, 1011–1023.

Williamson, A., Wickliffe, K.E., Mellone, B.G., Song, L., Karpen, G.H., and Rape, M. (2009). Identification of a physiological E2 module for the human anaphase-promoting complex. Proc. Natl. Acad. Sci. USA *106*, 18213–18218.

Wu, T., Merbl, Y., Huo, Y., Gallop, J.L., Tzur, A., and Kirschner, M.W. (2010). UBE2S drives elongation of K11-linked ubiquitin chains by the anaphase-promoting complex. Proc. Natl. Acad. Sci. USA *107*, 1355–1360.

Wu-Baer, F., Lagrazon, K., Yuan, W., and Baer, R. (2003). The BRCA1/BARD1 heterodimer assembles polyubiquitin chains through an unconventional linkage involving lysine residue K6 of ubiquitin. J. Biol. Chem. *278*, 34743–34746.

Ye, Y., Scheel, H., Hofmann, K., and Komander, D. (2009). Dissection of USP catalytic domains reveals five common insertion points. Mol. Biosyst. *5*, 1797–1808.

Ye, Y., Akutsu, M., Reyes-Turcu, F., Enchev, R.I., Wilkinson, K.D., and Komander, D. (2011). Polyubiquitin binding and cross-reactivity in the USP domain deubiquitinase USP21. EMBO Rep. *12*, 350–357.

Zhu, X., Ménard, R., and Sulea, T. (2007). High incidence of ubiquitin-like domains in human ubiquitin-specific proteases. Proteins *69*, 1–7.